EMBO reports

EMBO open

scientific report

Crystal structure and ligand binding of the MID domain of a eukaryotic Argonaute protein

Andreas Boland, Felix Tritschler, Susanne Heimstädt, Elisa Izaurralde[+] *& Oliver Weichenrieder*[++]

Department of Biochemistry, Max Planck Institute for Developmental Biology, Tübingen, Germany

Argonaute (AGO) proteins are core components of RNA-induced silencing complexes and have essential roles in RNA-mediated gene silencing. They are characterized by a bilobal architecture, consisting of one lobe containing the amino-terminal and PAZ domains and another containing the MID and PIWI domains. Except for the PAZ domain, structural information on eukaryotic AGO domains is not yet available. In this study, we report the crystal structure of the MID domain of the eukaryotic AGO protein QDE-2 from *Neurospora crassa*. This domain adopts a Rossmann-like fold and recognizes the 5′-terminal nucleotide of a guide RNA in a manner similar to its prokaryotic counterparts. The 5′-nucleotide-binding site shares common residues with a second, adjacent ligand-binding site, suggesting a mechanism for the cooperative binding of ligands to the MID domain of eukaryotic AGOs.

Keywords: GW182; miRNAs; RNAi; silencing; siRNAs

EMBO *reports* (2010) **11**, 522–527. doi:10.1038/embor.2010.81

INTRODUCTION

Proteins of the Argonaute (AGO) family have essential roles in RNA-mediated gene silencing mechanisms throughout the eukaryotic lineage. They associate with small non-coding RNAs to form RNA–protein effector complexes called RNA-induced silencing complexes (Tolia & Joshua-Tor, 2007; Jínek & Doudna, 2009). In RNA-induced silencing complexes, the small RNA functions as a sequence-specific guide that directs AGOs to fully or partially complementary target RNAs through base pairing interactions. The target RNA is then silenced at the transcriptional or post-transcriptional level (Tolia & Joshua-Tor, 2007; Jínek & Doudna, 2009).

Department of Biochemistry, Max Planck Institute for Developmental Biology, Spemannstrasse 35, Tübingen D-72076, Germany

[+]Corresponding author. Tel: +49 7071 601 1350; Fax: +49 7071 601 1353; E-mail: elisa.izaurralde@tuebingen.mpg.de

[++]Corresponding author. Tel: +49 7071 601 1358; Fax: +49 7071 601 1353; E-mail: oliver.weichenrieder@tuebingen.mpg.de

Received 30 March 2010; revised 10 May 2010; accepted 12 May 2010; published online 11 June 2010

Structural and biochemical studies showed that AGOs consist of four domains: an amino-terminal domain; a PIWI/Argonaute/Zwille (PAZ) domain that binds to the 3′-end of guide RNAs; the middle (MID) domain that provides a binding pocket for the 5′-phosphate of guide RNAs; and the P-element-induced whimpy testes (PIWI) domain that adopts an RNaseH fold and has endonucleolytic activity in some but not all AGOs (Parker *et al*, 2004, 2005, 2009; Song *et al*, 2004; Ma *et al*, 2005; Yuan *et al*, 2005; Wang *et al*, 2008a,b, 2009). Thus far, structural information on full-length AGOs is only available for the homologous proteins from archaea and eubacteria (Song *et al*, 2004; Ma *et al*, 2005; Parker *et al*, 2005; Yuan *et al*, 2005; Wang *et al*, 2008a,b, 2009), which can use DNA instead of RNA as guide molecules (Ma *et al*, 2005; Parker *et al*, 2005; Yuan *et al*, 2005; Wang *et al*, 2008a,b, 2009).

The function of AGO, however, has only been studied in eukaryotic systems; and, in the microRNA (miRNA) pathway, the precise mechanism by which AGO proteins mediate translational repression of target messenger RNAs (mRNAs) remains controversial (Eulalio *et al*, 2008a). Understanding such silencing mechanisms requires detailed structural information about the domains of eukaryotic AGOs; however, so far, this level of information is only available for the PAZ domain (Lingel *et al*, 2003; Song *et al*, 2003; Yan *et al*, 2003).

In this study, we focused on the structure of a eukaryotic AGO MID domain, because it is thought to perform essential and distinct functions in the miRNA pathway and because a considerable amount of discussion has focused on the MID domain fold (Kiriakidou *et al*, 2007; Kinch & Grishin, 2009; Djuranovic *et al*, 2010). Furthermore, it has been proposed that certain eukaryotic AGO MID domains sequester the mRNA 5′-cap structure (m^7GpppN) of target mRNAs, thereby repressing translation. Initially, this idea was based on the observation that the human AGO2 binds to m^7GTP Sepharose beads (Kiriakidou *et al*, 2007). Recent data by Djuranovic *et al* (2010) supported this concept, indicating that, in addition to the 5′-phosphate-binding pocket for the guide RNA, *Drosophila melanogaster* AGO1 has a second miRNA-dependent site that can bind to nucleotides such as the 5′-cap.

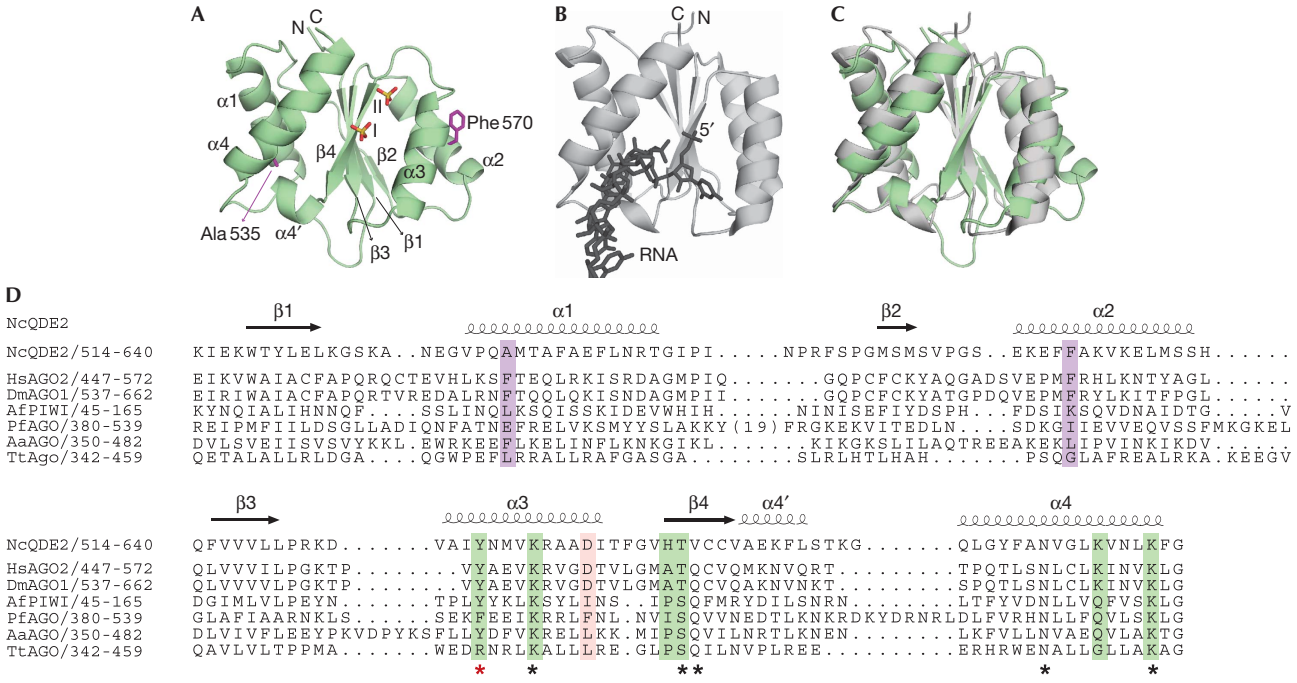

Fig 1 | Structure of the *Neurospora crassa* QDE-2 MID domain. (**A**) Ribbon representation of the MID domain showing the positions of two bound sulphate ions (I and II) as sticks (red: oxygen; yellow: sulphur). Residues corresponding to those proposed by Kiriakidou *et al* (2007) to sandwich the m^{7}GpppN cap are shown as purple sticks. Secondary structure elements are labelled. (**B**) Ribbon representation of an *Af* MID domain in complex with the 5′-end of a guide RNA (sticks), generated from Protein Data Bank entry 2bgg (Parker *et al*, 2005). (**C**) Superposition of the *Nc* QDE-2 MID domain onto the *Af* MID domain, illustrating the conservation of the Rossmann-like fold. (**D**) Structure-based sequence alignment of the *Nc* QDE-2 MID domain with archaeal (*Af*, *Pf*) and eubacterial (*Aa*, *Tt*) homologues, as well as with eukaryotic MID domains involved in the miRNA pathway. Positions involved in coordinating the two sulphate ions are shown in green. Positions proposed by Kiriakidou *et al* (2007) to bind the m^{7}GpppN cap are shown in purple. The position proposed by Djuranovic *et al* (2010) to effect allosteric regulation of miRNA binding is shown in pink. Invariant or highly conserved positions are marked by an asterisk. *Aa*, *Aquifex aeolicus*; *Af*, *Archaeoglobus fulgidus*; MID, middle; miRNA, micro RNA; *Nc*, *Neurospora crassa*; *Pf*, *Pyrococcus furiosus*; QDE-2, quelling deficient 2; *Tt*, *Thermus thermophilus*.

Kiriakidou *et al* (2007) proposed that eukaryotic AGO MID domains fold in a eukaryotic initiation factor 4E (eIF4E)-like manner, sandwiching the m^{7}GpppN cap between two phenylalanine residues (Marcotrigiano *et al*, 1997). By contrast, Djuranovic *et al* (2010) modelled the MID domain onto the Rossmann-like fold of the archaeal and eubacterial homologues. This latter modelling lead the authors to propose allosteric control of cap binding by the presence of the guide RNA 5′-nucleotide in a conserved binding pocket corresponding to that observed in the prokaryotic MID domains.

In this study, we present the crystal structure of the *Neurospora crassa* quelling deficient 2 (QDE-2) MID domain (Fulci & Macino, 2007) as an example of a eukaryotic AGO MID domain. This structure convincingly refutes the idea that eukaryotic MID domains adopt an eIF4E-like fold and shows the guide RNA 5′-phosphate-binding site is conserved. Furthermore, we describe a second, previously unreported ligand-binding site that allows a simple mechanistic explanation for the allosteric effects reported by Djuranovic *et al* (2010).

RESULTS

Structure of a eukaryotic AGO MID domain

The 2.2 Å structure of the *N. crassa* AGO MID domain (*Nc* QDE-2 MID; residues Lys 514–Gly 640) was solved by experimental phasing using a selenomethionine-substituted protein and was refined with excellent stereochemistry (supplementary Table S1 online). The protein adopts a Rossmann-like fold with a central four-stranded parallel β-sheet sandwiched between α-helices in a βαβαβαβαα topology (Fig 1A–D). The structure superimposes well with the structures of previously determined archaeal and eubacterial AGO MID domains, despite the low sequence identity (Fig 1C,D). Among the best-scoring structural relatives is the AGO MID domain from *Archaeoglobus fulgidus* (*Af*; Protein Data Bank (PDB) ID: 1w9h), showing an r.m.s.d. value of 2.6 Å and a sequence identity of 9%. For comparison, the r.m.s.d./sequence identity is 2.2 Å/16% for *Aquifex aeolicus* (*Aa*; PDB ID: 1yvu), 2.7 Å/12% for *Pyrococcus furiosus* (*Pf*; PDB ID: 1u04) and 3.3 Å/14% for *Thermus thermophilus* (*Tt*; PDB ID: 3ho1). By contrast, the sequence identities for eukaryotic homologues are generally greater than 20% (24% for *Homo sapiens* (*Hs*) AGO2, 26% for *D. melanogaster* (*Dm*) AGO1; Fig 1D). The structure of the *Nc* QDE-2 MID domain thus serves as a prototype for eukaryotic AGO MID domains.

The *Nc* QDE-2 MID domain structure has no similarity to eukaryotic eIF4E. Consequently, it is unlikely that eukaryotic AGO MID domains sandwich the m^{7}GpppG mRNA 5′-cap between two aromatic amino-acid side chains in an eIF4E-like

manner. In our structure, the two residues (Ala 535 and Phe 570) corresponding to those proposed to be important for cap binding (Kiriakidou *et al*, 2007) lie more than 25 Å apart (Fig 1A, purple). Earlier sequence analyses and homology modelling reached similar conclusions (Kinch & Grishin, 2009; Djuranovic *et al*, 2010). Furthermore, in previous studies, we showed that double valine substitutions of these residues abolished the silencing activity of *Dm* AGO1 and *Hs* AGO2 by preventing the interaction with both miRNAs and the GW182 protein, which is essential for miRNA-mediated silencing in animal cells (Eulalio *et al*, 2008b).

The 5′-phosphate-binding pocket is highly conserved

Several archaeal AGO proteins have been crystallized in complex with a guide RNA/DNA (Ma *et al*, 2005; Parker *et al*, 2005; Yuan *et al*, 2005; Wang *et al*, 2008a,b, 2009). The respective structures reveal that the 5′-terminal nucleotide of the guide molecule is not available for base pairing with the RNA target but is strongly bent and accommodated in a preformed pocket of the MID domain (Fig 1B). In each case, the base stacks onto an aromatic or arginine side chain (Fig 1D, red asterisk). Most importantly, the 5′-terminal phosphate (a hallmark of small interfering RNAs and miRNAs) is coordinated precisely by several side-chain and main-chain contacts to residues from helix α3, strand β4 and helix α4 (supplementary Fig S1A,B online; Parker *et al*, 2005; Wang *et al*, 2009). Furthermore, in the context of full-length proteins, the carboxyl terminus of the PIWI domain contacts the 5′-phosphate through a metal ion (Parker *et al*, 2005; Wang *et al*, 2009).

When a binary complex containing the *Af* MID and PIWI domains plus a guide RNA (PDB ID: 2bgg; Parker *et al*, 2005) is superposed onto the *Nc* QDE-2 MID domain, the 5′-terminal uridine of the guide RNA is positioned favourably into its positively charged binding pocket, with the base stacking on the aromatic ring of Tyr 595 of the *Nc* QDE-2 MID domain and the 5′-phosphate being coordinated by the Tyr 595 hydroxyl group (Fig 2A,B). Most importantly, the 5′-phosphate superimposes almost perfectly with a sulphate ion (ion I; from the crystallization conditions) that is coordinated additionally by the invariant lysines Lys 599 (helix α3) and Lys 638 (helix α4), as well as by the main-chain nitrogen of Cys 612 (strand β4) and the poorly conserved Lys 634 (helix α4; Fig 2A,B). Conversely, a superposition of the *Nc* QDE-2 MID domain onto the structures of *Af* or *Tt* MID domains places the sulphate ion (I) at the position of the 5′-phosphate of the guide RNA or DNA, respectively; this illustrates that the ligand-binding residues are conserved structurally (supplementary Fig S1A,B online). We conclude that eukaryotic AGO MID domains accommodate the 5′-terminal nucleotide of the guide RNA in a manner similar to their archaeal and eubacterial counterparts.

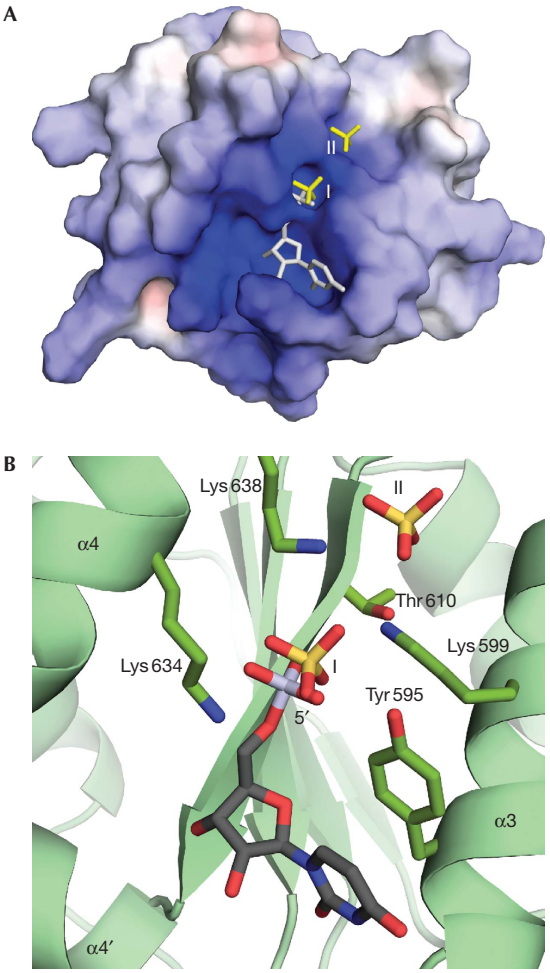

Fig 2 | Conservation of the guide RNA 5′-nucleotide-binding pocket. (**A**) Electrostatic potential mapped onto the molecular surface of the *Nc* QDE-2 MID domain, with the two bound sulphates shown as yellow sticks. Potentials are contoured from −10 (red) to +10 kT/e (blue). The 5′-RNA nucleotide from the superposition with the *Af* MID domain in complex with a guide RNA (Fig 1B,C) is shown as grey sticks. (**B**) Close-up of the RNA 5′-end nucleotide-binding site. The superimposed 5′-uridine from the *Af* complex structure is shown as sticks, together with the two sulphates and important side chains from the *Nc* QDE-2 structure. The uridine base stacks on the aromatic Tyr 595 ring, whereas the 5′-phosphate superimposes with sulphate I. Red: oxygen; blue: nitrogen; yellow: sulphur; violet: phosphorus. *Af*, *Archaeoglobus fulgidus*; MID, middle; *Nc*, *Neurospora crassa*; QDE-2, quelling deficient 2.

A second ligand-binding pocket

The structure of the *Nc* QDE-2 MID domain contains a second sulphate ion (II), only 6.3 Å from the first ion; this second ion is also well coordinated (Fig 3A,B). This second ligand-binding pocket is separated from the first 5′-phosphate-binding pocket by only two invariant lysines, Lys 599 and Lys 638, which thus participate simultaneously in coordinating both sulphate ions (Fig 3A,B). The second sulphate ion is coordinated further by the main-chain and side-chain atoms from Thr 610 (strand β4), which is invariantly a serine or threonine, and by the non-conserved side-chain of His 609 (strand β4; Fig 3A,B). As a consequence, the two sulphate-binding pockets are not independent of each other, but are likely to display positive cooperativity (that is, a ligand binding to either would orient the lysines favourably and promote binding of a ligand to the other site).

The presence of two positively coupled ligand-binding sites on the *Nc* AGO MID domain is particularly interesting in the context of a recent report by Djuranovic *et al* (2010), indicating

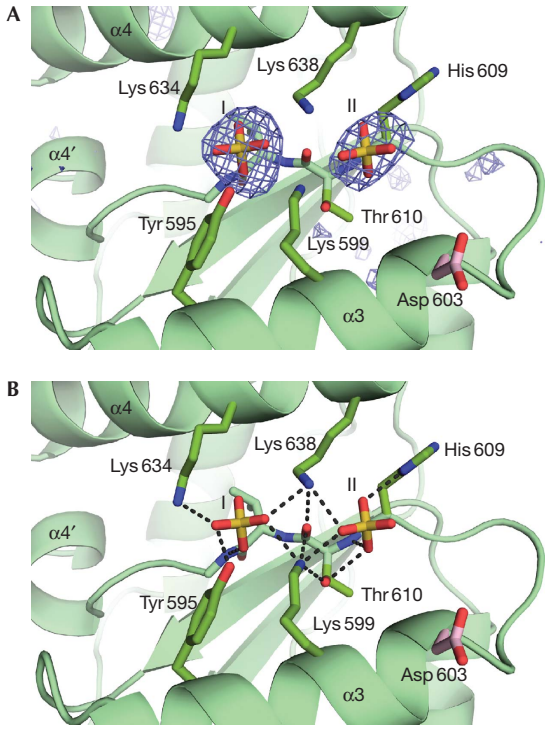

Fig 3 | Coupled coordination of the two sulphate ion ligands. (**A**) Difference density for the sulphate ions. Difference density ($(|F_o|-|F_c|)e(i\alpha_c)$) is contoured at 3.0 sigma values over the mean, where $|F_o|$ is the observed structure factor amplitudes and $|F_c|$ and α_c are structure factor amplitudes and phases calculated from a model prior to including the sulphates. (**B**) Potential hydrogen bonds of the two sulphate ions (I and II) to side-chain and main-chain atoms of the *Nc* QDE-2 MID domain. Relevant side chains and the main chain of strand β4 are shown as sticks. Hydrogen bonds are shown as dotted lines. Asp 603 (pink) corresponds to the aspartate proposed by Djuranovic *et al* (2010) to effect allosteric regulation of miRNA binding. Red: oxygen; blue: nitrogen; yellow: sulphur. MID, middle; miRNA, micro RNA; *Nc*, *Neurospora crassa*; QDE-2, quelling deficient 2.

that miRNA binding to the MID domain of *Dm* AGO1 might be under allosteric control (Djuranovic *et al*, 2010). These authors suggested that the MID domains of certain eukaryotic AGOs (that is, those involved in miRNA-mediated gene regulation) contain a second nucleotide-binding site in addition to the 5′-phosphate-binding pocket, which gains affinity for m^7GpppG cap analogues (or eventually for other ligands) only in the presence of the guide-strand RNA (and vice versa). It is thus tempting to speculate that the second sulphate ion observed in the context of the *Nc* QDE-2 MID domain could occupy such a second ligand-binding site.

Ligand binding by the two sites is expected to be cooperative. Accordingly, *Dm* AGO1b binding to miRNAs, m^7GpppG cap analogue and GW182 protein was abrogated by substituting the invariant tyrosine residue in the first binding site (*Dm* AGO1b residue Tyr 619, corresponding to *Nc* QDE-2 Tyr 595) or swapping the charge of an aspartic residue in the second ligand-binding site (*Dm* AGO1b residue Asp 627, corresponding to *Nc* QDE-2 Asp 603; Djuranovic *et al*, 2010). The inhibitory effect of the D627K substitution on miRNA binding is surprising because this residue is distant from the miRNA-binding site (Djuranovic *et al*, 2010). The equivalent residue in the *Nc* QDE-2 MID domain Asp 603 is located less than 7 Å away from the second sulphate (Fig 3A,B). Consequently, the Asp 627 side chain of *Dm* AGO1b could indeed participate in binding a ligand that superimposes with the second sulphate.

DISCUSSION

The structure of the *Nc* QDE-2 MID domain suggests that AGO proteins could be regulated by positive cooperativity of distinct ligands. Indeed, the structure reveals two precisely coordinated sulphate ions in adjacent binding pockets. Two highly conserved lysines (Lys 599 and Lys 638) coordinate both sulphates simultaneously and are thus shared by both binding pockets. Clearly, the first of the two sulphates on the *Nc* QDE-2 MID domain occupies the binding pocket for the 5′-terminal phosphate of the miRNA/short interfering RNA. The second sulphate is coordinated directly by three of the six most highly conserved side chains in AGO MID domains (that is, T(S)610, Lys 599 and Lys 638; Fig 1D). These residues are conserved not only in sequence but also in their structural orientation in bacterial and archaeal MID domains (supplementary Fig S1A,B online). Thus, the second sulphate might mark an ancient second (allosteric) binding site that has evolved different specificities in different AGO homologues (for example, for the cap structure, GW182 or other ligands).

We cannot predict what the ligand for the second binding site might be for different AGOs, because the properties and accessibility of this second binding site would depend on the orientation and the nature of the side chains provided by the PIWI domain. Indeed, in the current structures of the archaeal and eubacterial proteins, the PIWI domain restricts access to the second ligand-binding site. Nevertheless, the situation might be different for the eukaryotic AGOs, as Djuranovic *et al* (2010) observed an allosteric effect between the two binding sites using protein constructs that contained the PIWI domain. For AGO proteins involved in the miRNA pathway, the second ligand-binding site was suggested to bind to the m^7GpppN cap structure, or residues from the GW182 protein (Djuranovic *et al*, 2010). In agreement with this hypothesis, substituting residues in either of the two binding pockets simultaneously abrogated *Dm* AGO1 binding to miRNAs, GW182 and m^7GpppG cap analogue (Djuranovic *et al*, 2010). However, other AGO proteins, such as *Nc* QDE-2, might have evolved to be regulated by distinct ligands or might no longer be regulated by a second ligand. Nevertheless, for those AGO proteins that show ligand-dependent regulation, the coupled participation of the invariant lysines, Lys 599 and Lys 638, in both ligand-binding sites would be an attractive and mechanistically simple explanation for the ligand-dependent regulation of AGO protein function.

METHODS

Cloning, protein expression, purification and crystallization. The sequence encoding the MID domain of *Nc* QDE-2 was amplified by PCR from a pBluescript-SK^+ plasmid containing the genomic sequence of the *qde-2* gene (provided by G. Macino) and subsequently inserted into the *Nco*I and *Not*I sites of

the pETM60 vector (derived from pET24d; Novagen) using the primer pairs: 5′-CATGCCATGGCAGTCAAGGTCGCCAGA CCTT-3′ (forward) and 5′-ATAAGAATGCGGCCGCTTAGATATTG TGATTGGTGCCGC-3′ (reverse).

The resulting NusA–6 × His–MID protein fusion was expressed in the *Escherichia coli* BL21 Star (DE3) strain (Invitrogen) at 20 °C overnight. Protein expression was induced with 1 mM isopropyl β-D-1-thiogalactopyranoside at an A_{600} of 0.6. The fusion protein was purified first by a Ni^{2+}-affinity step. The removal of the NusA and polyhistidine tags was done by proteolytic digestion using tobacco etch virus protease at 4 °C overnight. The MID domain was purified further by heparin affinity chromatography and subsequent gel filtration (HiLoad 26/60 Superdex 75 pg; GE Healthcare). Finally, the QDE-2 MID domain was concentrated to 25 mg per ml in 10 mM HEPES (pH 7.2), 150 mM NaCl and 1 mM DTT.

Crystalline clusters of native and selenomethionine-substituted QDE-2 MID domain were grown by hanging drop vapour diffusion over a 500 µl reservoir at 18 °C. The protein solution described above was mixed 1:1 with various solutions containing 16–30% polyethylene glycol 4000 and 150–250 mM ammonium sulphate. Crystals were optimized by microseeding and flash-frozen in liquid nitrogen in the respective reservoir solution supplemented with 10 or 15% glycerol for cryoprotection.

Data collection, structure solution and refinement. Diffraction data were recorded on a PILATUS 6M detector (Broennimann *et al*, 2006) at the beamline PXII of the Swiss Light Source at a wavelength of 1.0 Å for the native data set and at the absorption peak of the selenomethionine derivative at 0.9792 Å. Diffraction images were processed with XDS (Kabsch, 1993). The crystals belong to space group $C222_1$, with one molecule per asymmetric unit and 52% solvent. The structure was solved from the selenomethionine data by single anomalous dispersion. AutoSHARP (Vonrhein *et al*, 2007) was used to search for five selenium sites per molecule. The assignment of the correct hand and solvent flattening was done automatically. ARP/wARP (Cohen *et al*, 2008) built a partial model comprising 99% of the backbone and 93% of the side chains docked correctly. The model was completed manually in COOT (Emsley & Cowtan, 2004) by using the native data. Refinement was done using Phenix (Adams *et al*, 2010) and COOT iteratively. The structure was validated with MOLPROBITY (Davis *et al*, 2007) and WHATCHECK (Hooft *et al*, 1996).

Accession codes. The coordinates of the MID domain have been deposited at the PDB with the accession code 2xdy.

Supplementary information is available at *EMBO reports* online (http://www.emboreports.org).

ACKNOWLEDGEMENTS

We thank G. Macino for providing *Neurospora crassa* QDE-2 plasmid DNA and R. Büttner for technical assistance. We thank the staff at the PX beamlines of the Swiss Light Source for assistance with data collection. This study was supported by the Max Planck Society, by grants from the Deutsche Forschungsgemeinschaft (FOR855 and the Gottfried Wilhelm Leibniz Program awarded to E.I.), and by the Sixth Framework Programme of the European Commission through the Silencing RNAs: Organisers and Coordinators of Complexity in Eukaryotic Organisms (SIROCCO) Integrated Project LSHG-CT-2006-037900.

CONFLICT OF INTEREST

The authors declare that they have no conflict of interest.

REFERENCES

Adams PD *et al* (2010) PHENIX: a comprehensive Python-based system for macromolecular structure solution. *Acta Crystallogr D Biol Crystallogr* **66:** 213–221

Broennimann C *et al* (2006) The PILATUS 1M detector. *J Synchrotron Radiat* **13:** 120–130

Cohen SX *et al* (2008) ARP/wARP and molecular replacement: the next generation. *Acta Crystallogr D Biol Crystallogr* **64:** 49–60

Davis IW *et al* (2007) MolProbity: all-atom contacts and structure validation for proteins and nucleic acids. *Nucleic Acids Res* **35:** W375–W383

Djuranovic S, Zinchenko MK, Hur JK, Nahvi A, Brunelle JL, Rogers EJ, Green R (2010) Allosteric regulation of Argonaute proteins by miRNAs. *Nat Struct Mol Biol* **17:** 144–150

Emsley P, Cowtan K (2004) COOT: model-building tools for molecular graphics. *Acta Crystallogr D Biol Crystallogr* **60:** 2126–2132

Eulalio A, Huntzinger E, Izaurralde E (2008a) Getting to the root of miRNA-mediated gene silencing. *Cell* **132:** 9–14

Eulalio A, Huntzinger E, Izaurralde E (2008b) GW182 interaction with Argonaute is essential for miRNA-mediated translational repression and mRNA decay. *Nature Struct Mol Biol* **15:** 346–353

Fulci V, Macino G (2007) Quelling: post-transcriptional gene silencing guided by small RNAs in *Neurospora crassa*. *Curr Opin Microbiol* **10:** 199–203

Hooft RW, Vriend G, Sander C, Abola EE (1996) Errors in protein structures. *Nature* **381:** 272

Jínek M, Doudna JA (2009) A three-dimensional view of the molecular machinery of RNA interference. *Nature* **457:** 405–412

Kabsch W (1993) Automatic processing of rotation diffraction data from crystals of initially unknown symmetry and cell constants. *J Appl Crystallogr* **26:** 795–800

Kinch LN, Grishin NV (2009) The human Ago2 MC region does not contain an eIF4E-like mRNA cap binding motif. *Biol Direct* **4:** 2

Kiriakidou M, Tan GS, Lamprinaki S, De Planell-Saguer M, Nelson PT, Mourelatos Z (2007) An mRNA m7G cap binding-like motif within human Ago2 represses translation. *Cell* **129:** 1141–1151

Lingel A, Simon B, Izaurralde E, Sattler M (2003) Structure and nucleic-acid binding of the *Drosophila* Argonaute 2 PAZ domain. *Nature* **426:** 465–469

Ma JB, Yuan YR, Meister G, Pei Y, Tuschl T, Patel DJ (2005) Structural basis for 5′-end-specific recognition of guide RNA by the *A. fulgidus* PIWI protein. *Nature* **434:** 666–670

Marcotrigiano J, Gingras AC, Sonenberg N, Burley SK (1997) Cocrystal structure of the messenger RNA 5′ cap-binding protein (eIF4E) bound to 7-methyl-GDP. *Cell* **89:** 951–961

Parker JS, Roe SM, Barford D (2004) Crystal structure of a PIWI protein suggests mechanisms for siRNA recognition and slicer activity. *EMBO J* **23:** 4727–4737

Parker JS, Roe SM, Barford D (2005) Structural insights into mRNA recognition from a PIWI domain–siRNA guide complex. *Nature* **434:** 663–666

Parker JS, Parizotto EA, Wang M, Roe SM, Barford D (2009) Enhancement of the seed-target recognition step in RNA silencing by a PIWI/MID domain protein. *Mol Cell* **33:** 204–214

Song JJ, Liu J, Tolia NH, Schneiderman J, Smith SK, Martienssen RA, Hannon GJ, Joshua-Tor L (2003) The crystal structure of the Argonaute2 PAZ domain reveals an RNA binding motif in RNAi effector complexes. *Nat Struct Mol Biol* **10:** 1026–1032

Song JJ, Smith SK, Hannon GJ, Joshua-Tor L (2004) Crystal structure of Argonaute and its implications for RISC slicer activity. *Science* **305:** 1434–1437

Tolia NH, Joshua-Tor L (2007) Slicer and the Argonautes. *Nat Chem Biol* **3:** 36–43

Vonrhein C, Blanc E, Roversi P, Bricogne G (2007) Automated structure solution with autoSHARP. *Methods Mol Biol* **364:** 215–230

Wang Y, Sheng G, Juranek S, Tuschl T, Patel DJ (2008a) Structure of the guide-strand-containing Argonaute silencing complex. *Nature* **456:** 209–213

Wang Y, Juranek S, Li H, Sheng G, Tuschl T, Patel DJ (2008b) Structure of an Argonaute silencing complex with a seed-containing guide DNA and target RNA duplex. *Nature* **456:** 921–926

Wang Y, Juranek S, Li H, Sheng G, Wardle GS, Tuschl T, Patel DJ (2009) Nucleation, propagation and cleavage of target RNAs in Ago silencing complexes. *Nature* **461:** 754–761

Yan KS, Yan S, Farooq A, Han A, Zeng L, Zhou MM (2003) Structure and conserved RNA binding of the PAZ domain. *Nature* **426:** 468–474

Yuan YR, Pei Y, Ma JB, Kuryavyi V, Zhadina M, Meister G, Chen HY, Dauter Z, Tuschl T, Patel DJ (2005) Crystal structure of *A. aeolicus* Argonaute, a site-specific DNA-guided endoribonuclease, provides insights into RISC-mediated mRNA cleavage. *Mol Cell* **19:** 405–419